



Cone-Beam Computed Tomographic Evaluation of the Posterior Wall of the Nasopharynx in Turkish Population

 Ceren Ozeren Keskek

Izmir Demokrasi University, Faculty of Dentistry, Department of Oral and Maxillofacial Radiology, İzmir, Türkiye

Content of this journal is licensed under a Creative Commons Attribution-NonCommercial-NonDerivatives 4.0 International License.



Abstract

Aim: This study aims to evaluate the radio-morphometry of important anatomical structures such as Rosenmüller fossa (RF), pharyngeal bursa (PB), and Eustachian tube (ET) in the posterior wall of the nasopharynx by cone beam computed tomography (CBCT).

Material and Methods: The posterior wall of the nasopharynx was analyzed retrospectively in CBCT images of 110 patients. The depth and width of the Rosenmüller fossa (RF), pharyngeal bursa (PB), and Eustachian tube (ET), their distances to the posterior nasal spina (PNS) and mid-sagittal plane, and the angles between them were measured. RF was categorized into three types. The relationship between the measured values and gender, age groups, and RF types was investigated. The obtained variables were analyzed statistically.

Results: The mean right RF depth was 8.2 and left RF was 8.6 mm. RF widths differed significantly by gender (right $p=0.013$, left $p=0.004$). There was a statistically significant positive correlation between RF-PNS distances and age (left $r=0.314$, $p=0.001$; right $r=0.240$, $p=0.011$). The prevalence of RF types was 31.8%, 19.5%, and 48.6% for type A, type B, and type C, respectively. In individuals with RF Type C, both RF and ET were located more lateral to the midline. The prevalence of PB was 45.5%.

Conclusion: Nasopharyngeal carcinoma (NPC) most commonly occurs in the RF. A good knowledge of the anatomy and variations of the nasopharyngeal region is important in the early diagnosis of NPC. Oral and maxillofacial radiologists must know the anatomy of the nasopharynx to understand and interpret incidental findings in CBCT.

Keywords: Cone-beam computed tomography, Eustachian tube, nasopharynx, nasopharyngeal carcinoma, pharyngeal bursa, Rosenmüller fossa.

INTRODUCTION

The posterior wall of the nasopharynx has important anatomical structures and consists of loose connective tissue (1). Some of these important anatomical structures are the pharyngeal recess (PR), the pharyngeal bursa (PB), and the Eustachian tube (ET). During nasotracheal intubation, if the end of the nasotracheal tube strikes the posterior wall of the nasopharynx, this can lead to retropharyngeal dissection and other serious complications (2). Being aware of the differences in the anatomy of the nasopharyngeal region can reduce the risk of such complications during nasotracheal intubation (1). In addition, it has been reported that calcific formations (3) such as rhinoliths, and structures such as Tornwaldt cysts (4), which are epithelial remnants of embryological origin, can be seen in this region.

Rosenmüller fossa (RF) also called lateral PR, was first reported by Johann Christian Rosenmüller. The RF is located just posterior to the torus tubarius, below the skull base, and extends laterally behind the ET orifice. Its location is important because there is only a thin layer of fibro connective tissue between it and the internal carotid artery (5). RF is lined with nasopharyngeal mucosa and is the most common area of nasopharyngeal carcinoma (NPC). NPC is most commonly seen in the 50-60 age group (6). Early diagnosis and treatment increase the survival rate of patients (7). The first symptom to appear on imaging of NPC is bluntness and asymmetry in RF (8). For this reason, it is very substantial for oral and maxillofacial radiologists to fully understand the anatomy of RF, which is the most common area of NPC (9).

While the posterior wall of the nasopharynx can only be

CITATION

Ozeren Keskek C. Cone-Beam Computed Tomographic Evaluation of the Posterior Wall of the Nasopharynx in Turkish Population. Med Records. 2023;5(Suppl 1):110-5. DOI:1037990/medr.1351878

Received: 29.08.2023 Accepted: 28.09.2023 Published: 09.10.2023

Corresponding Author: Ceren Ozeren Keskek, İzmir Demokrasi University, Faculty of Dentistry, Department of Oral and Maxillofacial Radiology, İzmir, Türkiye

E-mail: cerenozeren35@gmail.com

seen with endoscopy, computed tomography (CT) allows the investigation of all anatomical features (2). Cone beam computed tomography (CBCT) is often utilized in dentistry to examine bone for dental implants and orthodontic treatment. It also allows the acquisition of noninvasive, accurate measurements and three-dimensional images of anatomical structures and spaces (10). The use of CBCT has many advantages such as low radiation dose, high bone resolution, ease of use, and accessibility (1).

This study aims to investigate the morphometric features of the anatomical structures including RF, PB, and ET in the posterior wall of the nasopharynx using CBCT.

MATERIAL AND METHOD

The study was approved by the Izmir Katip Çelebi University Non-Interventional Clinical Studies Ethics Committee (IRB:26.05.2022,262) in accordance with the Helsinki Declaration of 1975, as revised in 2013. Informed consent was obtained from individuals before the CBCT procedure.

Sample size calculation was done using G*Power 3.1.9.7 software with 0.693 effect size, 5% significance level, 0.95 power. CBCT images of 110 random patients taken for assorted reasons (Dental Trauma, implant planning, examination of impacted teeth, orthodontic treatment planning, etc.), at the Department of Oral and Maxillofacial Radiology, Faculty of Dentistry, Izmir Katip Çelebi University were evaluated. Inclusion criteria were the patient's age over 18, high-quality CBCT images, and clear visualization of the nasopharynx. Patients with craniofacial deformity or syndrome, pathological formation in the nasopharynx region, the presence of any artifact that may interfere with the interpretation of the image and a history of surgery and trauma in the relevant region were not included in the study.

All CBCT images used were acquired with a CBCT device (NewTom 5G, Quantitative Radiology, Verona, Italy) shooting at 110 kVp. Images with a voxel size of 0.200 mm and a FOV range of 15x12 cm were used. CBCT images were evaluated in dim light conditions using a 27-inch screen size monitor (Eizo Radiforce MX270W - EIZO Corp.; Ishikawa, Japan) at 2560x1440 resolution and computer software NNT Viewer version 8.0 (NewTom - Quantitative Radiology; Verona, Italy). All measurements were made by one observer - oral and maxillofacial radiologist.

Reference points (posterior nasal spina (PNS) and basion (Ba)), RF, and ET orifice are shown in Figure 1 in the CBCT axial section. For measurements, an axial view with PNS (the posterior most point of the bony hard palate in the mid-sagittal plane) and Ba (The midline point of the anterior border of the foramen magnum) in the same frame was chosen. Reference points (PNS and Ba) in the oropharynx were determined based on another study (10).

In the axial section, the depth, width, length, distance from the PNS, the distance to the mid-sagittal plane and the angle between the sagittal plane of the RF and ET recesses were measured (Figure 2). The presence or absence of PB

was noted. If PB was present, its depth and width were measured in the axial section and its length was measured in the sagittal section (Figure 3). RF is classified into three types(2): type A, depth <5 mm; type B, depth \geq 5 mm and width <1 mm; and type C, depth \geq 5 mm and width \geq 1 mm (Figure 4). All measurements were made bilaterally.

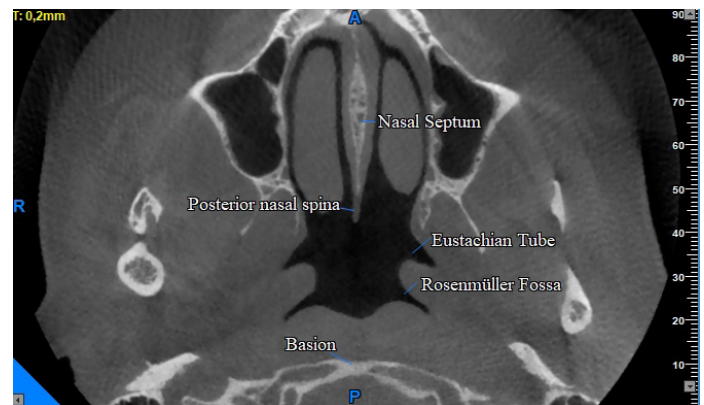


Figure 1. Anatomical structures of the nasopharynx in CBCT axial sections. Position of reference points (Posterior nasal spina and basion), Eustachian tube orifice, and Rosenmüller fossa

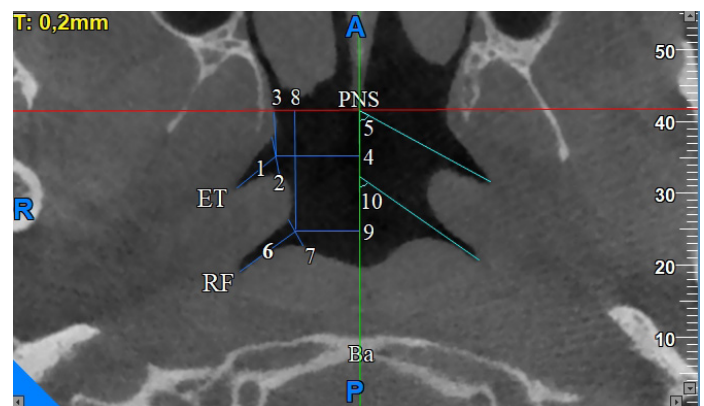


Figure 2. The measurements of Rosenmüller fossa (RF) and Eustachian tube (ET) orifice in axial section. 1, ET depth; 2, ET width; 3, ET-PNS distance; 4, ET-Mid-sagittal plane distance; 5, ET-Mid-sagittal plane angle; 6, RF depth; 7, RF width; 8, RF-PNS distance; 9, RF- Mid-sagittal plane distance; 10, RF-Midsagittal plane angle



Figure 3. The pharyngeal bursa (PB) measurements on CBCT images: (a) depth and width of PB in axial section, (b) length of PB in sagittal section

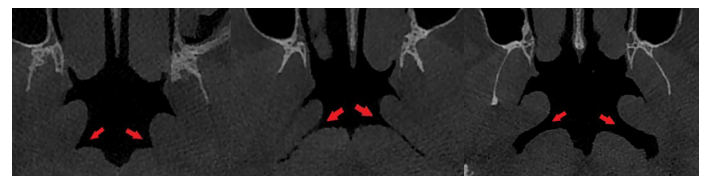


Figure 4. The classification of Rosenmüller fossa in axial section. (a) Type A, shallow fossa (<5 mm deep), (b) Type B, deep fossa (\geq 5 mm) with <1 mm wide openings, (c) Type C, deep fossa (\geq 5 mm) with \geq 1 mm wide openings

Statistical Analysis

All data were analyzed using the IBM SPSS Statistics Version 26.0 package program (IBM Corp.; Armonk, New York, USA). The conformity of the data to the normal distribution was evaluated with the Shapiro-Wilk test. Differences between normally distributed group means were analyzed using the t-test and one-way ANOVA. Tukey test was used in pairwise comparison tests of normally distributed variables. The relationship between normally distributed variables was defined using the Pearson correlation coefficient. In the comparison of qualitative variables, the number of observations (n) and their ratios (with the % values) were shown and the relationship between them was compared using the Chi-square test. The significance level was accepted as 0.05.

RESULTS

This study was performed retrospectively using CBCT images of 110 patients (57 females, 53 males) with a mean age of 44.68 years.

Measurements related to RF, and comparisons according to gender, age groups, and RF types are given in Table 1. While no statistically significant relationship was found between RF depths and gender ($p>0.05$), there was a significant relationship between RF widths and gender

($p<0.05$). In addition, there was a statistically significant difference between RF-PNS distances and age groups ($p<0.05$). Pairwise comparison results showed that the RF-PNS distance of individuals aged 51 and older increased significantly compared to individuals aged 18-35 ($p<0.05$). In addition, it was observed that the RF-PNS distance of individuals aged 51 and older increased compared to individuals aged 36-50 years, but this increase was not significant ($p>0.05$).

The prevalence of RF types A, type B and type C was 31.8%, 19.5%, and 48.6%, respectively, in a total of 220 RFs. The prevalence of right RF type A, type B and type C was 32.7%, 19.1%, and 48.2%, and the prevalence of left RF was 31%, 20%, and 49%, respectively.

Measurements related to ET and their comparisons according to gender and age groups are presented in Table 2. While the right ET-midsagittal plane distance was statistically significantly higher in men, the left ET-midsagittal plane angle was higher in women ($p<0.05$). Bilateral ET depths and ET-Midsagittal plane distances were statistically significantly higher in individuals with RF type C than in those with type A ($p<0.05$).

The prevalence and dimensions of PD according to gender are given in Table 3. RF-PNS distances were positively correlated with age (Table 4).

Table 1. The Rosenmüller fossa dimensions in axial section according to gender/age groups/RF types

		MEAN±SD									
	N	R-RF depth	R-RF width	R-RF-PNS	R-RF-MID	R-RF-angle	L-RF depth	L-RF width	L-RF-PNS	L-RF-MID	L-RF-angle
Gender											
Female	57	8.3±5.3	2.5±1.5	15.5±3.4	8.2±2	50.4±8.6	9.1±5	2.8±1.5	15.5±3.5	8.2±2.3	50.5±8.9
Male	53	8.1±5.4	1.9±1.2	14.8±3.7	8.7±2.5	51±12.2	8.1±5.6	2.1±1.2	15.2±3.6	7.5±1.7	51.3±12.9
p value		0.829	0.013*	0.299	0.245	0.750	0.331	0.004**	0.713	0.093	0.708
Age											
18-35	36	7.4±5.5	1.8±1.2	13.9±3.1 ^a	8.6±1.7	48.2±11.6	8.1±5.6	2.2±1.3	13.8±3.5 ^a	8.2±2.8	47.8±11.7
36-50	32	9.3±5.7	2.3±1.4	15.1±4.1 ^{ab}	8±1.8	49.9±10.3	9.5±5.9	2.6±1.3	15.4±3.5 ^{ab}	7.4±1.8	52.5±11.4
51+	42	8±4.9	2.5±1.6	16.3±3.3 ^b	8.8±2.9	53.3±9.1	8.3±4.5	2.5±1.6	16.7±3 ^b	7.9±1.8	52.3±9.6
p value		0.352	0.138	0.009***	0.288	0.087	0.498	0.437	0.001***	0.274	0.125
Total	110	8.2±5.3	2.2±1.4	15.2±3.6	8.5±2.3	50.7±10.5	8.6±5.3	2.5±1.4	15.4±3.4	7.9±2.1	50.9±11
RF type											
	N (R-L)										
Type A	36-34	2±2.4 ^a	2.3±1.4 ^a	14.4±3.7	7.2±1.8 ^a	43.6±11.1 ^a	2.3±1.8 ^a	2.7±1.5 ^a	14.7±3.6	6.5±1.5 ^a	42.5±12.2 ^a
Type B	21-22	10.4±3.4 ^b	0.8±0.4 ^b	15.2±3	8.5±1.8 ^{ab}	53.5±8.9 ^b	10.2±3.3 ^b	0.9±0.6 ^b	16.3±3.5	8.4±1.6 ^b	56.2±9.2 ^b
Type C	53-54	11.5±3.3 ^b	2.7±1.4 ^a	15.7±3.7	9.3±2.4 ^b	54.3±8 ^b	11.9±3.6 ^b	2.9±1.4 ^a	15.4±3.4	8.5±2.1 ^b	53.9±7.6 ^b
p value		0.000***	0.000***	0.257	0.000***	0.000***	0.000***	0.000***	0.224	0.000***	0.000***
Total	220	8.2±5.3	2.2±1.4	15.2±3.6	8.5±2.3	50.7±10.5	8.6±5.3	2.5±1.4	15.4±3.4	7.9±2.1	50.9±11

RF: rosenmuller fossa, PNS: posterior nasal spina, *Statistically significant at level $P\leq 0.05$ (independent samples t test), **Statistically significant at level $P\leq 0.01$ (independent samples t test), ***Statistically significant at level $P\leq 0.01$ (one way ANOVA), The lowercase superscript indicates statistical differences within column

Table 2. The orifice of the Eustachian tube dimensions in axial section according to gender/age groups/RF types											
MEAN±SD											
	N	R-RF depth	R-RF width	R-RF-PNS	R-RF-MID	R-RF-angle	L-RF depth	L-RF width	L-RF-PNS	L-RF-MID	L-RF-angle
Gender											
Female	57	5.2±1.8	4.7±1.1	6.1±2.4	11.3±1.7	53±7.3	5.1±1.7	4.7±1	6.5±2.5	11.2±1.3	51.3±8.2
Male	53	4.8±1.4	4.9±1.2	6.9±2.9	12.2±1.8	51.7±8	4.9±1.4	4.9±1.3	7.1±2.9	11.4±1.4	48.1±8.6
p value		0.168	0.381	0.123	0.012*	0.347	0.380	0.341	0.224	0.401	0.050*
Age											
18-35	36	4.4±1.4	4.5±1.2	6±2.9	11.8±1.8	50.9±9	5±1.6	4.6±1.2	6.3±2.8	11.5±1.3	46.7±8.5 ^a
36-50	32	4.9±1.6	4.7±1.2	6.6±2.8	11.7±1.9	53.3±5.3	5±1.4	4.9±1.2	6.8±2.9	11.2±1.4	50.9±7.7 ^{ab}
51+	42	5.5±1.7	5±1.2	6.8±2.4	11.6±1.8	52.9±7.9	5±1.7	4.7±1.1	7.1±2.5	10.8±1.4	51.6±8.6 ^b
p value		0.690	0.155	0.432	0.903	0.373	0.998	0.535	0.411	0.658	0.029*
Total	110	5±1.6	4.7±1.2	6.5±2.7	11.7±1.8	52.4±7.6	5±1.6	4.8±1.2	6.8±2.7	11.3±1.4	49.8±8.5
RF type N (R-L)											
Type A	36-34	4.3±1.4 ^a	4.8±1.1	6.4±2.4	11.1±1.7 ^a	50±7.8	4.4±1.3 ^a	4.3±1.1	7±3	10.8±1.3 ^a	48.5±7.8
Type B	21-22	4.9±1.5 ^{ab}	4.7±1.3	6.1±2.7	11.7±1.2 ^{ab}	53.6±7.5	5.3±1.6 ^{ab}	5.2±1.3	7.1±2.7	11.2±1.2 ^{ab}	49.6±10.4
Type C	53-54	5.5±1.6 ^b	4.7±1.1	6.5±2.8	12.1±1.9 ^b	53.4±7.3	5.2±1.5 ^b	4.8±1	6.4±2.4	11.5±1.3 ^b	50.6±8.1
p value		0.003***	0.930	0.890	0.038**	0.076	0.022**	0.007*	0.479	0.039**	0.552
Total	220	5±1.6	4.7±1.2	6.5±2.7	11.7±1.8	52.4±7.6	5±1.6	4.8±1.2	6.8±2.7	11.3±1.4	49.8±8.5

RF: rosenmuller fossa, PNS: posterior nasal spina, *Statistically significant at level $P \leq 0.05$ (independent samples t test), **Statistically significant at level $P \leq 0.05$ (one way ANOVA), ***Statistically significant at level $P \leq 0.01$ (one way ANOVA), The lowercase superscript indicates statistical differences within column

Table 3. The relationship between the incidence and dimensions of pharyngeal bursa with gender						
	PB Presence N (%)	PB Absence N (%)	Total N (%)	PB depth Mean (SD)	PB width Mean (SD)	PB length Mean (SD)
Female	29 (26.4)	28 (25.4)	57 (51.8)	3.8 (1.4)	4.3 (2.5)	5.7 (1.9)
Male	21 (19.1)	32 (29.1)	53 (48.2)	4.1 (1.1)	4.6 (1.8)	6.8 (2.6)
Total	50 (45.5)	60 (54.5)	110 (100)	3.9 (1.3)	4.4 (2.2)	6.2 (2.2)
p value		0.236		0.400	0.551	0.093

PB: Pharyngeal Bursa

Table 4. The comparison of Rosenmüller fossa and posterior nasal spina distance by age		
	R-RF-PNS	L-RF-PNS
r	0.240*	0.314**
Age	p	0.011
	n	110

RF: rosenmuller fossa, PNS: posterior nasal spina, *Correlation is significant at the 0.05 level (2-tailed), **Correlation is significant at the 0.01 level (2-tailed)

DISCUSSION

In the literature, the anatomical structures of the posterior wall of the nasopharynx were examined using computed tomography (CT) (2,11-13) and CBCT (1,7-9). CBCT provides accurate and reliable measurements of bone tissue. CBCT has advantages such as shorter scanning times, lower costs, and a lower radiation dose (14). The CBCT technology allows scanning with the patient in an

upright position (7). Sutthiprapaporn et al. (10) evaluated RF depth in supine and upright positions using computed CT and CBCT. They argued that when in an upright position, the tissues surrounding the RF may fall under the influence of gravity, causing the RF to appear deeper. They reported that in 83% of cases, the RF was deeper when the position was changed from the supine to the upright position. They measured the right and left RF depths of 9.8±6.6 mm and 6.8±6.5 mm, respectively, in images acquired in the upright position using CBCT. In this study, right and left RF depths were measured as 8.2±5.3 mm and 8.6±5.3 mm, on CBCT images obtained in the supine position. The RF depths measured in this study were like those measured using CBCT by Sutthiprapaporn et al. (10). This contradicts the argument that RF will be imaged less deeply by taking CBCT in the supine position. There is a need for different comparative studies in which the sample size is increased.

NPC is a rare tumor arising from the epithelial lining of the nasopharynx. RF is the most common origin of NPC. Its incidence is higher in men (6). The pathogenesis of NPC is not clear. It is estimated that there are many risk factors such as the Epstein-Barr virus, genetic factors, and nutrition (15). Hoe (13) retrospectively analyzed CT images of 56 patients with biopsy-proven NPC to investigate the origins and extent of NPC. Hoe (13) reported that the first NPC lesion appeared in the RF area and this tumor spread to the adjacent parapharyngeal area in 64% of the cases. In another study, Hoe analyzed CT images of 60 patients with biopsy-proven NPC and reported that levator veli palatini muscle was thickened and RF was blunt in all these patients (12). Therefore, it is important to know the mean measurement values of the anatomical structures in the posterior nasopharyngeal wall and their relationship with age and gender for the early diagnosis of infiltrates and possible pathologies.

Some early symptoms and signs of NPC, such as ear, face, and headache, and trismus, may be confused with symptoms of temporomandibular dysfunction (TMD) (15). Özyar et al. (16) found that 5 percent of patients had trismus at the time of diagnosis of NPC. Zubizarreta et al. (17) declared that trismus was the first sign of NPC in up to 36% of patients. The possibility of NPC should also be evaluated in patients who are diagnosed with TMD. For this reason, RF, where NPC is most common, should be meticulously investigated for bluntness and asymmetries in CBCT images. During these CBCT examinations, oral maxillofacial radiologists may have a substantial role in the early recognition of NPC. In cases where doubts increase, patients should be directed to the necessary medical doctors (8).

Nasotracheal intubation is a potentially traumatic procedure. Takasugi et al. (2) reported that in wide-opened RFs (Type C), the nasotracheal tube may impinge on the posterior wall of the nasopharynx, resulting in possible retropharyngeal laceration and even dissection. In their study, type C was detected in 24% of cases. In this study, 48.6% of the total 220 RFs were type C. Type C with a high rate indicates that the regional anatomy should be well known for each patient to reduce the potential risks. An interesting finding in our study was that both ET and RF were located more lateral to the midline in individuals with RF type C than in those with RF type A. It can be thought that this may reduce the risk of injury or laceration.

Serindere et al. (7) reported that RF depth was statistically significantly higher in women. In our study and other studies (1,8,11), no significant difference was found in RF depth according to gender. In our study, the width of R-RF was 2.5 mm in females and 1.9 mm in males, and the width of L-RF was 2.8 mm in females and 2.1 mm in males. There is a statistically significant difference in RF width by gender. We obtained equivalent results with another study investigating the relationship between RF width and gender (1). While Kaplan et al. (1) did not report a significant difference in L-RF-PNS distance according to age groups, they found a difference between groups in

R-RF-PNS distance. In our study, there was a significant difference according to age groups in both L-RF-PNS and R-RF-PNS distances. In the correlation analysis, there was a positive correlation between age and RF-PNS distances.

The PB is a congenital blind sac located in the midline of the nasopharynx near the lower end of the pharyngeal tonsils (18). Takasugi et al. (2) determined the prevalence of PB as 16% in their study and reported that it is very unlikely to cause nasopharyngeal laceration during nasotracheal intubation since their openings are narrow. Kaplan et al. (1) reported the prevalence of PB as 40% in their study of 150 patients. In our study, the prevalence of PB was 45.5%, which is higher than in previous studies.

This study had several limitations. The study was conducted on CBCT data obtained from single center in the supine position. This situation prevents comparisons of both regional and ethnic differences. This study only performed morphometric analysis on CBCT images retrospectively. A clinical examination of the patients was not performed, and demographic information was not obtained. In future studies, demographic information on patients can be obtained, and comparisons can be made using CBCT data from different centers in the supine and upright positions.

CONCLUSION

In conclusion, there are few studies in the literature about the posterior wall of the nasopharynx, which contains important anatomical structures, including the RF, which is the most common site of NPC. Although CBCT is not used in practice for the diagnosis of NPC, it is frequently used for various purposes in dentistry. Dentists, and especially oral and maxillofacial radiologists, should be aware of these structures that can enter the imaging field, albeit incidentally, and have adequate anatomical knowledge to perform their responsibilities. A good knowledge of regional anatomy and its variations is particularly important for distinguishing pathologies. Further studies comparing different imaging modalities and positions with larger sample sizes may provide useful information.

Financial disclosures: The authors declared that this study has received no financial support.

Conflict of Interest: The authors declare that they have no competing interest.

Ethical approval: Ethical approval was obtained from İzmir Katip Çelebi University Non-Interventional Clinical Studies Ethics Committee (IRB:26.05.2022,262).

Acknowledgments: The author would like to thank Assoc. Prof. Emre Aytuğar for his help in providing data.

REFERENCES

1. Kaplan FA, Saglam H, Bilgir E, et al. Radiological evaluation of the recesses on the posterior wall of the nasopharynx with cone-beam computed tomography. Niger J Clin Pract. Jan;25:55-61.

2. Takasugi Y, Futagawa K, Konishi T, et al. Possible association between successful intubation via the right nostril and anatomical variations of the nasopharynx during nasotracheal intubation: a multiplanar imaging study. *J Anesth*. 2016;30:987-93.
3. Aksakal C. A very rare localization of rhinolith: fossa of rosenmuller. *J Craniofac Surg*. 2020;31:e113-4.
4. Alshuhayb Z, Alkhamis H, Aldossary M, et al. Tornwaldt nasopharyngeal cyst: case series and literature review. *Int J Surg Case Rep*. 2020;76:166-9.
5. Amene C, Cosetti M, Ambekar S, et al. Johann Christian Rosenmüller (1771-1820): a historical perspective on the man behind the fossa. *J Neurol Surg B Skull Base*. 2013;74:187-93.
6. Velayutham P, Davis P, Savery N, Vaigundavasan R. A common symptom with an uncommon diagnosis. *The Egyptian Journal of Otolaryngology*. 2021;37:95.
7. Serindere G, Gunduz K, Avsever H, Orhan K. The anatomical and measurement study of rosenmüller fossa and oropharyngeal structures using cone beam computed tomography. *Acta Clin Croat*. 2022;61:177-84.
8. Erdem Ş, Zengin AZ, Erdem Ş. Evaluation of the pharyngeal recess with cone-beam computed tomography. *Surg Radiol Anat*. 2020;42:1307-13.
9. Temiz M, Duman SB, Abdelkarim AZ, et al. Nasopharynx evaluation in children of unilateral cleft palate patients and normal with cone beam computed tomography. *Sci Prog*. 2023;106:368504231157146.
10. Sutthiprapaporn P, Tanimoto K, Ohtsuka M, et al. Improved inspection of the lateral pharyngeal recess using cone-beam computed tomography in the upright position. *Oral Radiology*. 2008;24:71-5.
11. Erdem H, Tekeli M, Cevik Y, et al. Quantitative assessment of the pharyngeal recess morphometry in anatolian population using 3D models generated from multidetector computed tomography images. *Med Records*. 2023;5:507-12.
12. Hoe J. CT of nasopharyngeal carcinoma: significance of widening of the preoccipital soft tissue on axial scans. *AJR Am J Roentgenol*. 1989;153:867-72.
13. Hoe JW. Computed tomography of nasopharyngeal carcinoma. A review of CT appearances in 56 patients. *Eur J Radiol*. 1989;9:83-90.
14. Scarfe WC, Farman AG, Sukovic P. Clinical applications of cone-beam computed tomography in dental practice. *J Can Dent Assoc*. 2006;72:75-80.
15. Reiter S, Gavish A, Winocur E, et al. Nasopharyngeal carcinoma mimicking a temporomandibular disorder: a case report. *J Orofac Pain*. 2006;20:74-81. Erratum in: *J Orofac Pain*. 2006;20:106.
16. Ozyar E, Ebru K, Ferah Y, Atahan İ. Factors related with development of treatment induced trismus in nasopharyngeal cancer patients. *Turkish Journal of Oncology*. 2006;21:57-62.
17. Zubizarreta PA, D'Antonio G, Raslawski E, et al. Nasopharyngeal carcinoma in childhood and adolescence: a single-institution experience with combined therapy. *Cancer*. 2000;89:690-5.
18. Ben Salem D, Duvillard C, Assous D, et al. Imaging of nasopharyngeal cysts and bursae. *Eur Radiol*. 2006;16:2249-58.